

Recent advances in optical MEMS devices and systems

P. R. Patterson, D. Hah, M. M. C. Lee, J.C. Tsai, and M.C. Wu

Electrical Engineering Department, University of California, Los Angeles
Room 63-128, Eng. IV Building, 405 Hilgard Ave., Los Angeles, CA 90095

ABSTRACT

We have developed novel optical micro-electro-mechanical systems, (MEMS) and nano-electro-mechanical, (NEMS) optical components for applications including imaging, switching, and optical integrated circuits. This paper provides an overview of current optical MEMS/NEMS research projects in our integrated photonics laboratory at UCLA. Three optical MEMS/NEMS devices: a large, 1 mm diameter, scanning micromirror for imaging applications, an analog micromirror array for network switching applications, and a nanoscale photonic crystal switch for integrated photonic circuit applications will be described.

Keywords: Angular Vertical Combdrive, Micromirrors, MEMS, NEMS, Optical scanner, Optical switch, Photonic crystal, Photonic Bandgap, SOI-MEMS, SUMMiT-V, WDM

1. INTRODUCTION

Micro-electro-mechanical systems, (MEMS), technology enables the creation of micro-optical elements which are inherently suited to cost effective manufacturability and scalability as the processes are derived from the very mature semiconductor microfabrication industry. Indeed, optical MEMS components have been successfully incorporated into commercial systems for displays¹ and more recently optical switches.^{2,3} The extremely rapid growth of optical MEMS technology driven by miniaturization, lightweight, low energy consumption, and reduced cost, is projected to continue in response to the demand for large scale optical switching in fiber optic networks.

While intensive efforts from industry over the last five years have facilitated the migration of many new optical MEMS components from research laboratories to commercial reality, research is ongoing to develop newer photonic MEMS components and technologies to address next and future generation photonic systems. In this paper we present the development of current optical MEMS research at UCLA with the description of three optical MEMS devices: a 1 mm diameter scanning micromirror with an angular vertical combdrive actuator⁴, an analog micromirror array with hidden vertical combdrive actuators⁵, and a nano-electro-mechanical photonic crystal switch.⁶ All three devices employ electrostatic combdrive actuation⁷: vertical combdrives actuate the micromirrors, and for the on/off photonic crystal switch, a lateral combdrive provides the motion between states. The optical components of these devices span a size range from millimeters to nanometers, a characteristic dictated by the specific optical application.

Optical imaging applications may require only one or two scanning micromirrors but the resolution is critical. In order to achieve ~1000 resolvable spots, the micromirror needs both a large optical aperture, (mirror diameter), and a large scan range. Our 1 mm diameter scanning micromirror has been developed for such an application. The analog micromirror array has been developed for free space switching of grating dispersed collimated beams and the mirror pitch of 150 μm is dictated by the design of the overall system.⁸ Such switching applications require less resolution; here the integration of many individual micromirrors with near identical scanning performance is important. Switching in the photonic crystal device requires silicon dimensions in the nanometer range corresponding to the quarter and full wavelength thickness from a 1.55 μm center wavelength.

Since MEMS are still a new microfabrication technology as compared to e.g., standard CMOS, considerable flexibility in both design and fabrication may be exercised to achieve the desired outcome. For the three devices presented here, we have utilized both, silicon-on-insulator, SOI-MEMS, processes developed at UCLA and a surface micromachined foundry process, Sandia ultra-planar multilevel MEMS technology-V, (SUMMiT-V). The motivations and advantages for the process technologies will be presented in the following sections for each device.

2. SCANNING MICROMIRROR WITH ANGULAR VERTICAL COMBDRIVE

As mentioned in the introduction, high resolution is a key parameter for imaging applications. Resolution as defined by number of resolvable spots is a function of the beam divergence and the scan range as shown in the following equations:

$$N = \frac{\theta_{\max}}{\delta\theta} \quad (1)$$

$$N \propto \frac{\theta_{\max} D}{\lambda} \quad (2)$$

Where: $\delta\theta$ is beam divergence, θ_{\max} is the maximum scan angle, D is the mirror diameter and λ is the wavelength of incident light.

In addition to high resolution, the micromirror should be optically smooth ($<\lambda/10$), and flat (radius of curvature $\sim 1\text{m}$).⁹ The single crystal silicon of SOI material is superior to deposited thin films since the surface is highly polished and there is little or no low residual stress. The actuator needs to be electrically fast (kHz range), have low operation voltage ($<100\text{V}$), and be capable of a large optical scan angle ($\pm 15^\circ$). For high speed scanning applications, electrostatic combdrive actuation has several advantages over parallel plate actuation. A relatively stiff torsion bar, required for high frequency operation, is feasible since more electrostatic force is generated by the large capacitance area and the narrow gap spacing between comb fingers providing more effective utilization of the driving voltage. Decoupling of the mirror and actuator permits a large deflection angle since the under mirror electrode is not required and the underside can be opened to accommodate a larger range of motion. In addition, the entire scan range is available since pull-in, (an unstable condition which renders the lower 60-70% of the gap spacing unusable in most parallel plate type scanners), can be avoided.

Vertical combdrives have been demonstrated, with a staggered vertical combdrive by patterning the fixed and moving teeth in distinct layers separated by sacrificial oxide¹⁰ or by adding a metal offset electrode on top of the fixed teeth.¹¹ The two layer staggered vertical combdrive requires critical alignment, although a 2-layer self-aligned process was reported recently.¹² Our approach, the angular vertical comb (AVC), features self-alignment between the fixed and moving teeth since the entire device is patterned with deep reactive ion etching, DRIE, in the top layer of a single SOI wafer. Furthermore our models shows that the AVC can achieve a 50% higher scan angle than a staggered vertical comb of equivalent dimensions due to the larger initial angle as shown in the schematic cross sectional views in Fig.1.

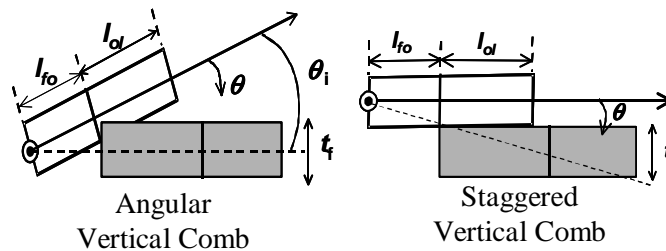


Figure 1. Schematic view of the angular vertical comb, (AVC), and the staggered vertical comb, (SVC), in the initial state.

The initial angle determines the maximum scan angle and is achieved by rotating the moving comb structure out of the wafer plane with a surface tension assembly technique driven by melting or reflowing photoresist.¹³ It can be shown that the maximum scan angle is directly proportional to the comb finger thickness and we have used SOI wafers with a 25 μm device layer.

The details of the fabrication process shown in Fig.2 have been published elsewhere.⁴ Briefly, the device is patterned into the top silicon layer with DRIE, an oxide is deposited and then opened in the regions where the photoresist hinges will attach, the backside is removed under the mirror with DRIE, the 9.5 μm photoresist hinge is patterned, the device is released in HF, the photoresist is reflowed in hot water, and finally a blanket metallization is deposited. Development of new processes to improve the planarity of the top layer is ongoing as photoresist residue in high aspect ratio structures after hinge patterning is difficult to remove and impacts the device yield by preventing the assembly of the moving comb teeth.

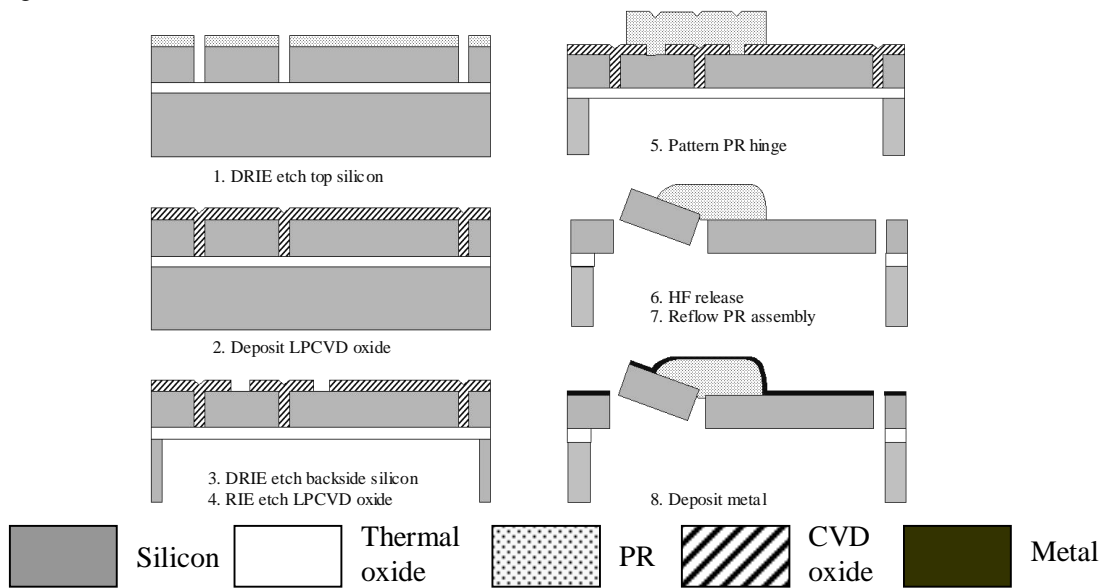


Figure 2. Process flow for angular vertical combdrive micromirror

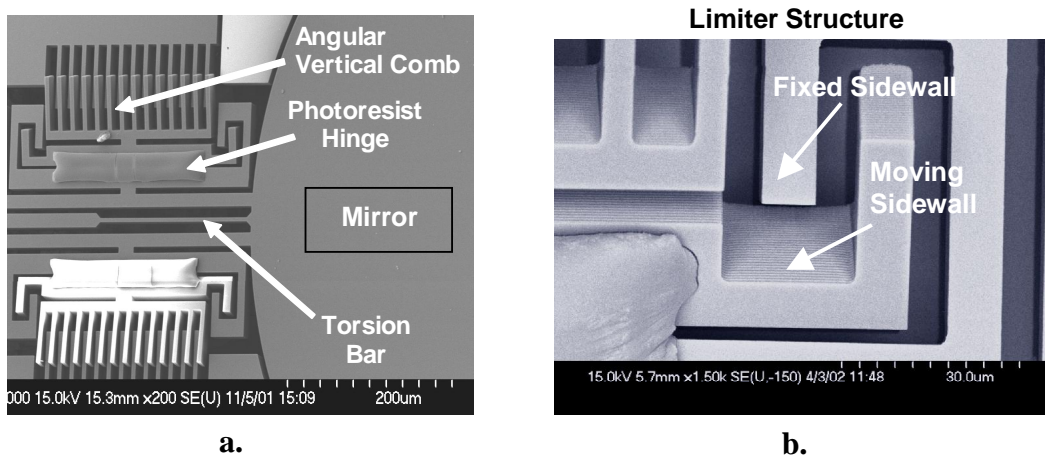


Figure 3. SEM images of a. scanning micromirror with AVC, b. detail of limiter structure

An SEM of the scanning micromirror with angular vertical combdrive is shown in Fig. 3a. The self assembled angle, (initial angle), of the moving comb is controlled by a physical stop or limiter as shown in Fig. 3b, the moving teeth and limiter arm are rotated out, (toward the viewer), until the moving sidewall hits the fixed sidewall and stops.

The mirror scan angle for a prototype device was found by measuring the static deflection, as a function of DC voltage, with a Wyko RTS 500 optical surface profiler. The maximum mechanical scan angle for the AVC scanner was found to be $\pm 1.6^\circ$ at 108V. Our theoretical models show that the DC performance can be further improved by using SOI starting material with a thicker device layer and by increasing the number of comb fingers. The resonant frequency for the scanning micromirrors was characterized with a Polytech Vibrascan laser doppler vibrometer. A resonant frequency of 1.4 kHz was measured for the device which is in good agreement with the calculated value of 1.44 kHz.

Deflection at resonance is significantly larger and we have measured an optical scan angle of $\pm 18^\circ$ with a 21V_{rms} sinusoidal input at 1.4 kHz. With this resonant scan angle and the mirror diameter of 1 mm, a resolution of ~960 resolvable spots is calculated for a wavelength of 633 nm. As stated previously, this is a key parameter for imaging applications where a few high resolution devices are required. The key parameters for the smaller scanning micromirrors of a switching array will be covered in the next section.

3. MICROMIRROR ARRAY WITH HIDDEN VERTICAL COMBDRIVE ACUATORS

Currently, the most anticipated application for optical MEMS components is in fiber optic communication networks. All-optical components eliminate the optical to electrical, (OE) conversion, and are therefore independent of transmission speed, protocol, and modulation format. Transparency to future changes in communication standards would be a distinct advantage in extending the life of such a system.¹⁴ Optical MEMS components with networking applications include: 2D³ and 3D¹⁵ MEMS optical switches and wavelength-division-multiplexed (WDM) optical add-drop multiplexers, (OADM).¹⁵

We have developed a 1 x 10 linear array of analog MEMS micromirrors for optical WDM routers and wavelength-selective crossconnect (WSXC) applications.⁵ The requirements for these applications include: high fill factor along the array direction to achieve a “flat-top” spectral response,¹⁷ minimum gap between the WDM channels, and a large continuous scan range to increase the number of fiber channels. In addition, low voltage and low power actuation are desired to reduce power consumption of the drive electronics.

As stated in the previous section, the vertical combdrive actuator^{9, 18} offers several inherent advantages for actuating micromirrors: specifically, a large continuous scan range since pull-in can be minimized or avoided, and a large force density allowing low voltage operation. However, single level processes such as the SOI-MEMS presented above, are not ideal. To achieve a high fill factor and maximize chip real estate the actuators are placed underneath the mirrors as shown schematically in Fig 4. The design is best achieved with the added flexibility of the multiple layers available in surface-micromachining fabrication processes.

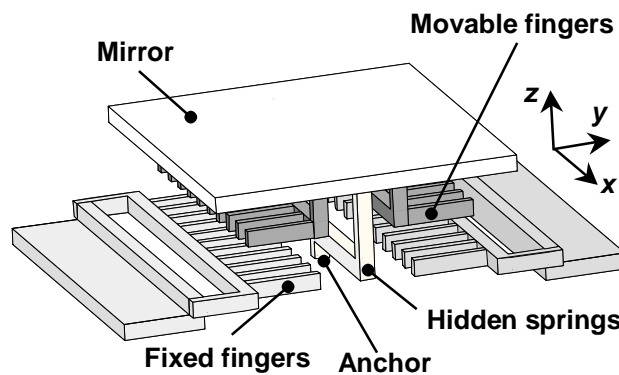


Figure 4. Schematic of single scanning mirror array element with hidden combdrive

The scanning array was fabricated with the Sandia ultra-planar multilevel MEMS technology V, SUMMiT-V process which consists of four structural polysilicon layers with planarized oxides between poly2 and poly3 and between poly3 and poly4. The combination of 4 polysilicon layers and the chemical mechanical planarization, CMP, of the oxide

layers make this process ideal for implementing these devices. The CMP process is critical for fabricating the hidden combdrives under the mirror as it prevents the transfer of the underlying topography to the mirror surface. The details of the device design including various spring configurations have been very recently reported.⁵ The spring is formed in poly1, the fixed fingers are formed with laminated poly1 (1 μm thick), and poly2 (1.5 μm thick), the moving fingers are formed in poly3 (2.25 μm thick), and the mirror is formed in poly4 (2.25 μm thick).

After fabrication the devices are released in HF and then metallized with Cr/Au by a maskless e-beam evaporation to increase the mirror reflectivity. Electrical isolation between electrodes is preserved by incorporating overhang structures in the design. SEM images of the mirror array and an individual scanner with one half of the mirror intentionally removed to reveal the underlying combdrive are shown in Fig. 5.

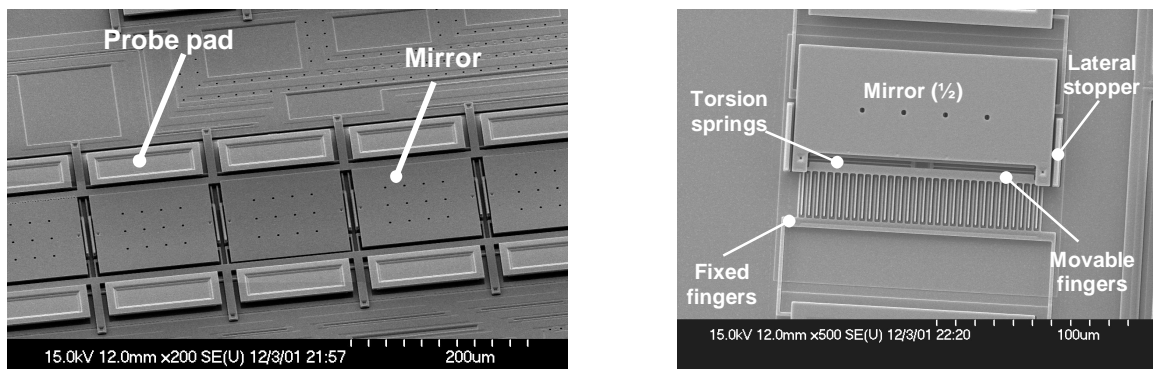


Figure 5. SEM images of the micromirror array (left), and an individual scanner with half the mirror intentionally removed to show underlying combdrive (right)

The mirror pitch of 150 μm is determined by the system requirement. With lateral stoppers, the maximum mirror width (x direction), allowed by SUMMiT-V design rules is 137 μm . Therefore, the linear fill-factor along the array direction is 91%. The mirror length (y direction), is 120 μm . The DC scanning characteristics of the micromirrors were measured with a Wyko RTS 500 optical surface profiler. Excellent uniformity across the array of scanning micromirror elements, ($< \pm 3.2\%$), has been measured as shown by the tight distributions in Fig. 6.

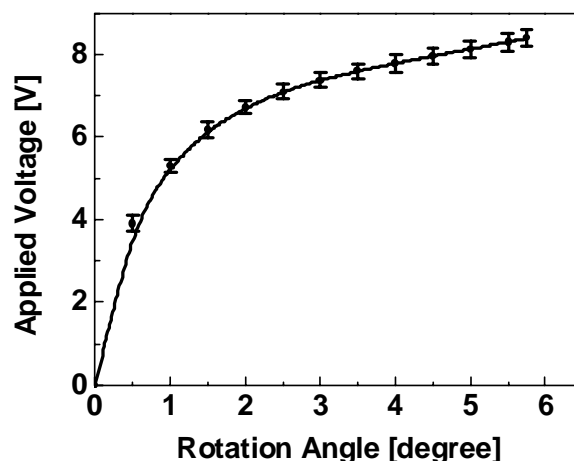


Figure 6. Uniformity of DC scanning characteristics in the 1×10 analog micromirror array

The device exhibits low operating voltage (6 V), wide scan range (23.6° optical), and moderate resonant frequency (3.4 kHz). In addition, crosstalk between adjacent mirrors was found to be below 20 dB. In the next section we will cover a switch of much smaller dimensions.

4. NANO-ELECTRO-MECHANICAL PHOTONIC CRYSTAL SWITCH

Photonic crystals, (PC), have the ability to confine light propagation within small volumes at specific frequency ranges, known as photonic bandgaps, (PBG). Narrow bandpass transmission spectra in the photonic bandgap can be created by inserting defects into the host PBG structure. In PC with a large index contrast between composite materials such as silicon and air, photonic bandgap filtering requires only a few periods and switching can be achieved by displacing these few photonic “atoms” to create a defect. Such structures provide very compact optical switching elements.

We have designed and fabricated a one-dimensional (1D), PBG switch that optically links silicon waveguides.⁶ The PC structure is sandwiched between input and output silicon waveguides as shown in Fig 7. An electrostatic actuator provides switching between two different PC structures: one which reflects the optical input and one which transmits the optical input. In the reflection state, the photonic crystal consists of silicon and air gaps designed at quarter wavelength thickness from a 1.55 μm center wavelength. This structure forms a bandstop filter, reflecting light with wavelengths in the range from 1.0 μm to 2.1 μm back into the input waveguide. When the actuator moves to the transmission state, a defect is formed by filling the gap with silicon. In this state the PC structure has a transmission resonance centered at 1.55 μm with a pass bandwidth ~ 70 nm and the light from the input waveguide is coupled to the output waveguide.

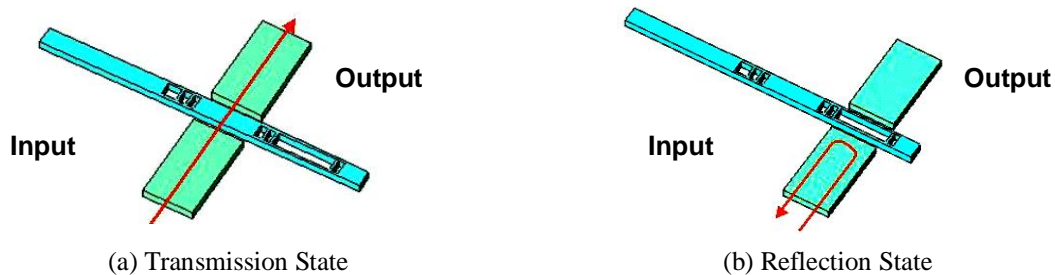


Figure 7. Schematic of 1D MEMS photonic crystal ON-OFF switch: (a) Transmission state, (b) Reflection state

A prototype photonic crystal device has been fabricated on an SOI wafer with a 1.5 μm device layer. An SOI process was chosen for the advantages the single crystal silicon provides: a flat structure with low residual stress for reliable nanostructure fabrication. The fabrication process combines electron beam direct write to define the nanoscale PBG structures, and optical lithography to define the larger actuators. All structures are created in a single DRIE etch step and are self-aligned. The minimum feature of the photonic crystal structure is 110 nm, (quarter wavelength thickness of Si for 1.55 μm), and therefore precise control of the lateral undercut during etching is very important.¹⁹ After etching, the structure is released in HF, followed by supercritical drying. A completed device is shown in Fig. 8.

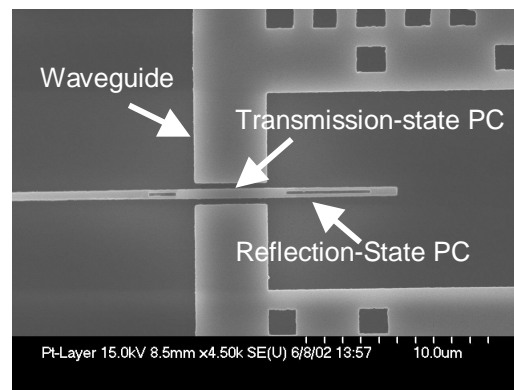


Figure 8. SEM of MEMS photonic crystal switch

The PBG switch was tested using a 1.55 μm laser to couple light into the waveguide via a lensed fiber. The peak wavelength in the transmission state was measured to be 1.56 μm , which is very close to the design wavelength of 1.55 μm . An extinction ratio of 11 dB was obtained between the transmission state and the reflection state for a 1.56 μm wavelength. A higher extinction ratio could be achieved with a single mode waveguide and polarization control. A switching time of less than 0.5 msec. was found for the temporal response shown in Fig. 8.

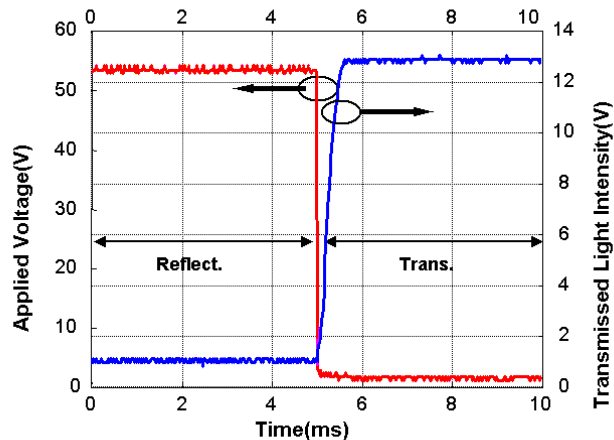


Figure 8. Temporal response of MEMS photonic crystal switch

5. CONCLUSION

Optical MEMS technology is an intensely active research area covering a broad range of applications which manipulate light in new ways. We have presented the details of our ongoing optical MEMS research projects by detailing the design, fabrication, and test results of three novel devices representative of the diverse applications and size range of optical MEMS devices today. In all cases MEMS is a key enabling technology for reconfigurable photonic circuits.

ACKNOWLEDGEMENTS

These UCLA projects are sponsored by DARPA under DAAH01-99-C-R220, N66001-00-C-8088, MDA972-00-1-0019, by NSF under BES-0119494, and by Agilent Technologies through the California MICRO program.

REFERENCES

1. L.J. Hornbeck, "Digital Light Processing and MEMS: Timely Convergence for a Bright Future", SPIE Micromachining and Microfabrication '95, plenary session, Austin, Texas, October 24, 1995.
2. V.A. Aksyuk, M.E. Simon, F. Pardo, S. Arney, D. Lopez and A. Villanueva "Optical MEMS Design for Telecommunications Applications", 2002 Solid-State Sensor and Actuator Workshop Tech. Digest, Hilton Head, SC, June 2-6, pp.1-6.
3. L. Fan, et al., "Digital MEMS switch for planar photonic crossconnects", OFC 2002 Tech. Digest, Anaheim, CA, March 17-22, 2002, p.93.
4. P. R. Patterson, D. Hah, H. Nguyen, R.-M. Chao, H. Toshiyoshi, and M. C. Wu, "A Scanning Micromirror with Angular Comb Drive Actuation", The 15th IEEE International Micro Electro Mechanical Systems Conference (MEMS 2002), Jan. 20- 24, 2002, Las Vegas, NV. p. 544-547.
5. D. Hah, S. Huang, H. Nguyen, H. Chang, J.-C. Tsai, and M.C.Wu, "Low Voltage MEMS Analog Micromirror Arrays with Hidden Vertical Comb-drive Actuators", 2002 Solid-State Sensor and Actuator Workshop Tech. Digest, Hilton Head, SC, June 2-6, 2002, pp.11-14.
6. M.-C. M. Lee, D. Hah, E. K. Lau, H. Toshiyoshi, M. Wu, "Nano-Electro-Mechanical Photonic Crystal Switches", OFC 2002 Tech. Digest, Anaheim, CA, March 17-22, 2002, p.94.
7. W.C. Tang, T-C. H. Nguyen, R.T. Howe, "Laterally Driven Polysilicon Resonant Microstructures", IEEE Proceedings Micro Electro Mechanical Systems, pp. 53-59, Feb. 1989.

8. D.Hah, S. Huang, H. Nguyen, H. Chang, and M.C.Wu, "A Low Voltage, Large Scan Angle MEMS Micromirror Array with Hidden Vertical Comb-drive Actuators for WDM Routers", OFC 2002 Tech. Digest, Anaheim, CA, March 17-22, 2002, p. 92.
9. S. Blackstone and T. Brosnihan, "SOI MEMS Technologies for Optical Switching", IEEE/LEOS International Conference on Optical MEMS, Okinawa, Japan, Sept. 25-28, 2001.
10. R. A. Conant, J.T. Nee, K. Lau, R.S. Mueller "A Flat High-Frequency Scanning Micromirror", 2000 Solid-State Sensor and Actuator Workshop Tech. Digest, Hilton Head, SC, June 4-8, 2000, pp. 6-9.
11. H. Schenk, P.Dürr, T. Hasse, D. Kunze, U. Sobe, H.Kück, "Large Deflection Micromechanical Scanning Mirrors for Linear Scans and Pattern Generation", IEEE Journal of Sel.Topics in Quantum Electronics, vol. 6, no.5, Sept./Oct. 2000, pp.715-722.
12. U. Krisnamoorthy and O. Solgaard, "Self-aligned Vertical Comdrive Actuators for Optical Scanning Micromirrors" 2001 International Conference on Optical MEMS, Okinawa, Japan,p.41.
13. R.R.A. Syms, C. Gormley, S. Blackstone, "Improving Yield, Accuracy and Complexity in Surface Tension Self-Assembled MOEMS", Sensors and Actuators A 88 (2001), pp.273-283.
14. L.Y. Lin, E.L. Goldstein, "Opportunities and Challenges for MEMS in Lightwave Communications", IEEE Journal on Sel.Topics in Quantum Electronics, Vol. 8, No. 1, Jan/Feb 2002, pp. 163-172.
15. R. Ryf, et al., "1296-port MEMS transparent optical crossconnect with 2.07Petabit/s switch capacity," Tech. Digest of the OFC 2001, Anaheim, CA, March 17-22, 2001, Postdeadline Paper PD28.
16. J. E. Ford, V. A. Aksyuk, David J. Bishop, and J. A. Walker, "Wavelength add-drop switching using tilting micromirrors," J. Light. Technol., vol. 17, (1999),pp.904-911.
17. J. S. Patel and Y. Silberberg, "Liquid crystal and grating-based multiple-wavelength cross-connect switch," IEEE Photon. Technol. Lett., 7, (1995), pp.514-516.
18. J.-L. A. Yeh, H. Jiang, and N. C. Tien, "Integrated polysilicon and DRIE bulk silicon micromachining for an electrostatic torsional actuator," J. Microelectromech. Syst., vol. 8, (1999), pp. 456-465.
19. Mikhail Naydenkov, Bahram Jalali, "Fabrication of High Aspect Ratio Photonic Bandgap Structures on Silicon-on-Insulator", Proceedings of the SPIE - The International Society for Optical Engineering, vol.3936, (Integrated Optics Devices IV, San Jose, CA, USA, 24-25 Jan. 2000.) SPIE-Int. Soc. Opt. Eng, 2000. p.33-9